International Journal of GEOMATE, March, 2026 Vol.30, Issue 139, pp.69-76
ISSN: 2186-2982 (P), 2186-2990 (O), Japan, DOI: https://doi.org/10.21660/2026.139.5349
Geotechnique, Construction Materials and Environment

THE EFFECT OF SEAM INCLINATION ON SURFACE SUBSIDENCE: A PARAMETRIC STUDY

*Ali Husain Taherdito[1], Hideki Shimada[1], Takashi Sasaoka[1], Akihiro Hamanaka[1] and Budi Sulistianto[2]

[1]Department of Earth Resources Engineering, Kyushu University, Japan; [2]Department of Mining Engineering, Institut Teknologi Bandung, Indonesia

*Corresponding Author, Received: 25 Nov. 2025, Revised: 25 Dec. 2025, Accepted: 26 Dec. 2025

ABSTRACT: Underground coal mining in inclined seams presents complex geomechanical challenges that differ significantly from horizontal strata, particularly regarding surface subsidence behavior. This study investigates the influence of seam inclination and panel geometry on the morphology of subsidence troughs using a 3D numerical modeling approach (FLAC3D). The model configuration is grounded in the specific operational conditions of a coal mine in East Kalimantan, Indonesia, utilizing a 16° seam inclination and site-specific lithology. A parametric study was conducted to evaluate the sensitivity of subsidence to panel width, depth, and height. The results reveal a distinct asymmetry in the subsidence profile driven by the tangential component of gravity along the bedding planes. Specifically, the locus of maximum subsidence shifts noticeably toward the down-dip direction, while the subsidence profile exhibits a steeper gradient on the up-dip side. Pearson correlation analysis quantifies the influence of geometric parameters, identifying extraction height as the governing variable ($\rho = 0.671$). Panel width demonstrates a moderate positive correlation ($\rho = 0.395$), whereas panel depth exhibits a weak inverse relationship ($\rho = -0.141$), functioning as a minor attenuating factor. The findings demonstrate that traditional symmetrical monitoring designs are insufficient for inclined seams. Consequently, this research suggests that subsidence management strategies in the Indonesian coal basin and similar geological settings must account for the down-dip shift of the maximum impact zone to ensure effective risk mitigation.

Keywords: Surface subsidence; Inclined seam; Parametric study; Strata propagation; Numerical simulation.

1. INTRODUCTION

Surface subsidence is an inevitable consequence of underground longwall mining, causing structural damage to infrastructure and disrupting utility networks. Beyond economic losses, these deformations alter surface water flow and trigger social tensions with local communities [1-4]. Therefore, accurate prediction of subsidence profiles is critical for effective risk management.

Historically, subsidence prediction relied on empirical and analytical techniques, such as influence functions and geometric assessments [5-8]. While valuable for simple geometries, these methods often struggle to account for complex geological conditions and rock mass heterogeneity. Consequently, recent research has shifted toward numerical modeling techniques (e.g., Finite Element and Finite Difference Methods) due to their ability to simulate complex strata mechanics and fault activation. For instance, Derbin successfully modeled deep mining-induced fractures using borehole-derived parameters, while Jeon utilized FLAC2D to integrate risk assessment with cavity geometry analysis [9-11]. Similarly, Xu employed finite difference modeling to assess sensitive surface structures [12], demonstrating the versatility of numerical approaches in capturing non-linear rock behavior.

Despite these advancements, prior numerical studies have predominantly focused on flat seam configurations. However, many operational coal fields, including those in Indonesia, feature dipping strata that significantly alter the subsidence mechanism. The influence of strata dip on the asymmetry of the subsidence trough has not been systematically evaluated in conjunction with mining geometry parameters. Research by Alejano provided foundational methodologies for inclined seams [13], but a comprehensive parametric study specifically targeting the interaction between seam inclination and panel geometry (width, depth, height) remains limited.

To address this gap, the numerical model developed in this investigation incorporates a seam inclination of 16°. This specific angle was selected to reflect the actual operational conditions of a case study mine in East Kalimantan, Indonesia. Although the regional average dip is approximately 12°, the targeted mining panel operates at a localized inclination of 16°. By modeling this specific configuration, this research serves as a pioneer study for the East Kalimantan coal basin, contributing valid data from a tropical geological setting that is currently underrepresented in global literature. This characterization is further achieved through a parametric study focusing on the panel's depth, width, and height.

2. RESEARCH SIGNIFICANCE

This research bridges a critical gap in geomechanical modeling by extending subsidence prediction beyond conventional flat-seam assumptions to address the complexities of inclined stratigraphy (16°). By grounding the simulation in the specific operational conditions of East Kalimantan, this study contributes valuable data to the underrepresented literature on Indonesian coalfields. Beyond its regional relevance, the study elucidates the mechanisms of asymmetrical trough formation and the lateral shift of maximum subsidence, providing a more accurate predictive framework for dipping seams globally. Furthermore, the identification of panel height as the governing variable offers vital guidelines for optimizing extraction parameters. These insights are essential for enhancing surface safety protocols and minimizing environmental impact in underground mining operations within inclined geological settings.

3. METHODOLOGY

3.1 Numerical Model Setup and Boundary Conditions

Three-dimensional numerical modeling was executed using FLAC3D to analyze a domain with dimensions of 420 m × 330 m × 555 m, as depicted in Fig. 1. The model configuration incorporates a single longwall panel with a length of 110 m, inclined at 16° to conform to the dip of the coal seam. The simulated stratigraphy comprises a coal seam overlain by soil, siltstone, sandstone, and claystone units, while the underlying strata predominantly consist of claystone.

To ensure computational accuracy, a mesh sensitivity analysis was conducted on a representative model configuration. Based on this analysis, the mesh was refined to a uniform size of 1 m in the region extending from the panel to the surface monitoring zone. This configuration provides a high vertical resolution of 10 elements across the seam height, ensuring detailed capture of strata deformation.

The model dimensions (420 m × 330 m) were selected based on both empirical field observations and theoretical influence zones. As evidenced by the field measurement data presented in Fig. 3, the actual surface subsidence basin in the study area dissipates and approaches zero displacement within a radius of approximately 200 m from the panel center. Since the numerical model extends 210 m from the center to the lateral boundary (half-width), the domain provides a sufficient buffer zone to accommodate the realistic subsidence trough observed in the field.

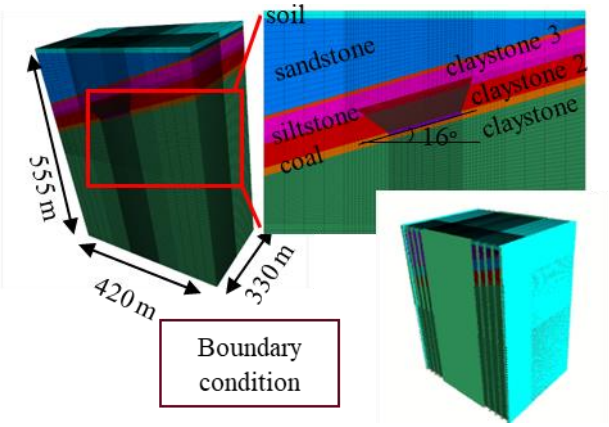

Fig. 1 The three-dimensional model construction

Boundary conditions constrained the lateral sides with roller boundaries (restricting horizontal displacement while permitting vertical movement), fully fixed the model base, and maintained a free surface at the top to facilitate vertical deformation analysis. Although specific simulation scenarios with substantial subsidence magnitudes (e.g., maximum panel width of 100 m or significant depths) exhibited minor residual vertical displacements at the model edges, these values are statistically negligible (less than 5% of the maximum subsidence). Therefore, they do not compromise the integrity of the analysis regarding the trough morphology and the lateral shift of the inflection points.

Fig. 2(c) demonstrates the final state of the model following the analysis. The simulation procedure encompasses model construction, initial equilibrium analysis (detailed in Fig. 2(a)), and sequential panel excavation in 10 m advancement steps. This stepwise approach was adopted to mitigate numerical instability associated with instantaneous large-scale excavation and to accurately capture the path-dependent stress redistribution characteristic of progressive mining operations.

Following excavation, the immediate roof collapse was simulated by replacing both the extracted panel and the overlying caved zone with a softer material [14-16]. The assumption of the caved zone height (Hc) is grounded in empirical observations for weak roof strata. According to Peng, the height of the immediate caved zone typically ranges from 2 to 8 times the mining height (H), depending on the bulking factor and lithological competence [17, 18]. Since the overburden in the study area consists predominantly of weak sedimentary rock, we adopted the upper bound value (Hc = 8H) to represent a scenario where the weak roof collapses readily and extensively fills the void. This assumption ensures that the model captures the full extent of the immediate roof disturbance.

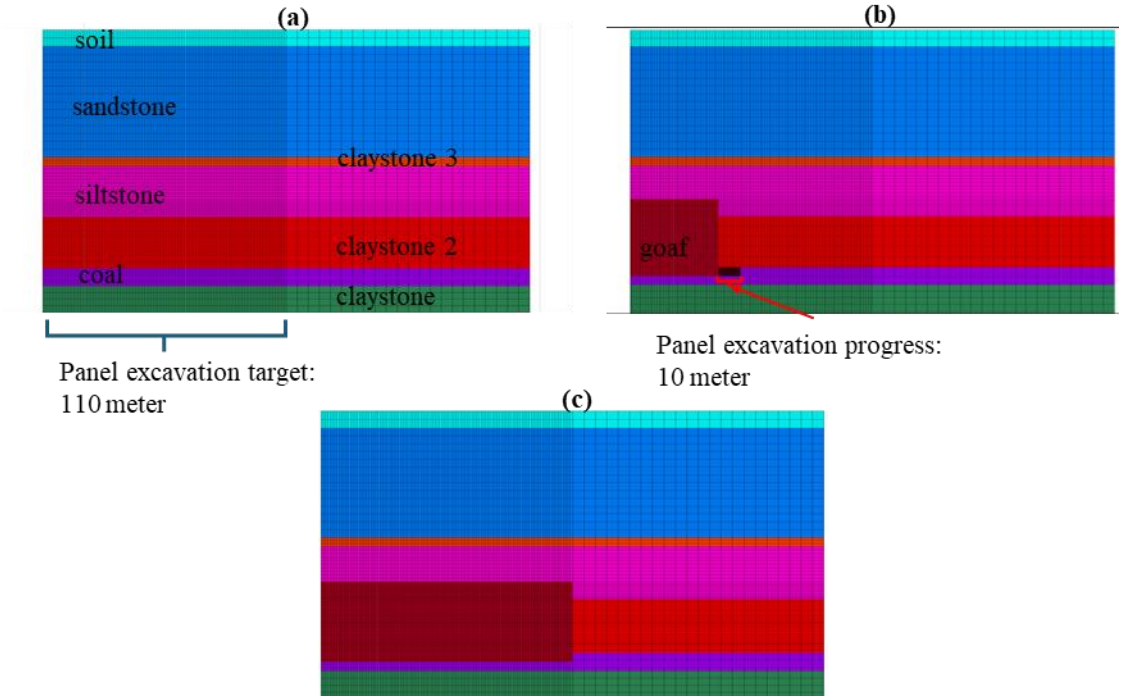

Fig. 2 (a) Initial model, (b) Excavation model, (c) Final model

3.2 Material Properties and Constitutive Model Justification

The material properties assigned to each geological stratum are detailed in Table 1. These parameters were derived from site-specific laboratory tests and incorporate seven distinct lithological units, including three claystone variations to account for depth-dependent strength increases. To address the transition from intact rock to rock mass, laboratory values were downscaled using the Geological Strength Index (GSI). The resulting parameters align with the typical weak, weathered strata characteristics of East Kalimantan. Goaf properties were adapted from regional studies on similar formations by Sasaoka with minor adjustments [19].

The Elastic-Perfectly Plastic Mohr-Coulomb constitutive model was selected for its computational efficiency and capability to capture shear failure zones and stress redistribution. While in-situ rock masses may exhibit strain-softening behavior, the perfectly plastic assumption remains a standard and robust approach for large-scale subsidence modeling. It provides a conservative estimate of strata deformation, which is sufficient for a parametric study aimed at identifying morphological trends rather than precise post-failure fragmentation.

Table 1. Material properties (source: internal laboratory test reports)

Zone group name	Unit Weight (MN/m^3)	Cohesion (MPa)	Friction Angle (°)	Young's modulus (MPa)	Poisson's ratio
Soil	0.016	0.016	22	20	0.35
Sandstone	0.022	0.805	43.83	672.1	0.24
Claystone3	0.021	0.703	30.2	1023.4	0.25
Claystone2	0.021	1.18	30.2	1856.8	0.27
Claystone	0.021	1.245	30.2	2899.9	0.26
Siltstone	0.021	0.856	35.6	1105.37	0.26
Coal	0.013	0.619	34.16	1512.88	0.36
Goaf	0.015	0.058	14.4	15.01	0.25

3.3 Parametric Study Design

Table 2. Simulation matrix parameter

Width	Depth	Height
55	100	3
70	145	5
100	200	10

Due to the computational complexity of integrating all operational variables, this study isolates the geometric attributes of the panel height, width, and depth as the primary independent variables. A comprehensive simulation matrix (Table 2) was established to evaluate parameter sensitivity. The study holds the seam dip (16°) and panel length (110 m) constant while varying three critical geometries: panel width (55, 70, and 100 m), depth (100, 145, and 200 m), and extraction height (3, 5, and 10 m).

Crucially, the 55 m width corresponds to the currently mined panel, providing a baseline for model validation, while the 70 m and 100 m widths represent design scenarios for future mine expansion. The systematic permutation of these variables yields a total of 27 distinct simulation scenarios for analysis.

4. NUMERICAL SIMULATIONS RESULTS

4.1 Model Validation Against Field Data

As demonstrated in Figs. 3 and 4, field measurements from East Kalimantan exhibit a distinctly asymmetrical profile, confirming the hypothesis that seam inclination governs trough morphology.

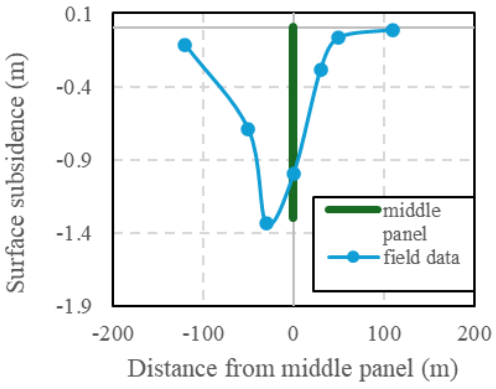

Fig. 3 Field subsidence measurements from an underground mine in East Kalimantan, Indonesia

The numerical model successfully reproduces this characteristic, accurately predicting the lateral shift of maximum subsidence (Smax) toward the down-dip direction and the steeper gradient observed on the up-dip side.

While a discrepancy in absolute magnitude exists, likely due to the exclusion of time-dependent compaction, the model demonstrates strong morphological agreement with field data. This confirms the validity of the underlying geomechanical mechanism, making the model suitable for a parametric study focused on identifying geometric trends and asymmetrical shifts rather than predicting precise site-specific magnitudes.

4.2 Effect of Stratigraphic Inclination

To quantify variations attributable to inclination, a comparative analysis between flat (0°) and inclined (16°) configurations was performed (Fig. 4). The simulation reveals two distinct behaviors. First, regarding trough geometry, the flat seam yields a symmetrical profile. In contrast, the inclined seam produces a marked asymmetry, characterized by a steeper gradient on the up-dip side and a broader slope on the down-dip side. Second, the location of Smax diverges significantly. Unlike the vertically aligned flat model, the inclined model exhibits a lateral shift of Smax toward the down-dip direction, deviating from the geometric center of the panel.

Fig. 5 elucidates the geomechanical mechanisms governing these behaviors. In the inclined model, strata deformation is driven by the resultant of gravitational forces and vectors perpendicular to the bedding planes. This causes the failure zone to propagate asymmetrically. Furthermore, the destressed zone (orange/red regions in Fig. 5) is skewed toward the down-dip boundary, disrupting the pressure arch equilibrium. Unlike the symmetrical load transfer in the flat model, the inclined configuration results in differential loading on the abutments, creating an asymmetrical stress distribution that dictates the surface subsidence profile.

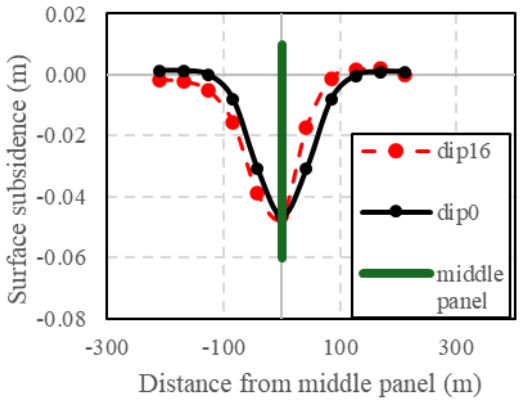

Fig. 4 Comparative analysis between a flat seam configuration (0°) and an inclined seam model (16°)

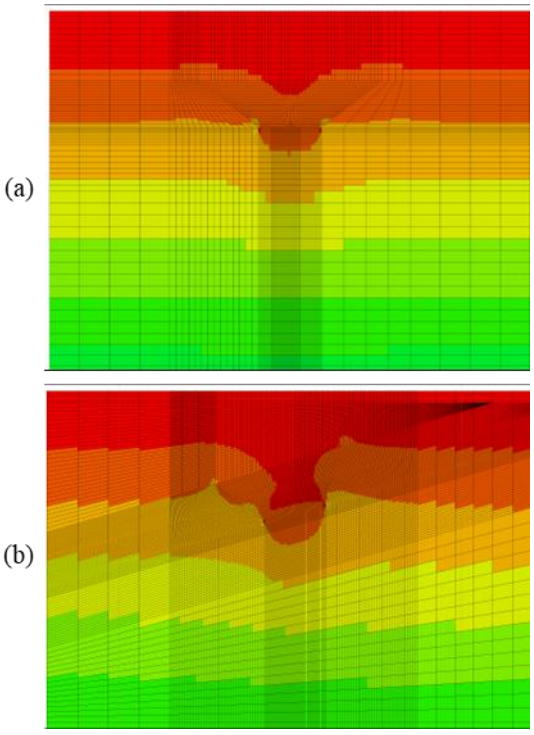

Fig. 5 (a) Post-excavation stress distribution flat seam model analysis (b) Post-excavation stress distribution inclination seam model analysis

4.3 Parametric Sensitivity Analysis

Table 3 summarizes the maximum vertical surface displacements for the 27 simulation scenarios. Results generally range from 0.009 m to 0.192 m, with a notable exception in Model 27 (1.6 m). This drastic outlier suggests that a critical stability threshold was exceeded. While other scenarios maintained an overburden bridging effect that limited surface deformation, the extreme geometry of Model 27 (100 m width, 100 m depth, 10 m height) caused a complete failure of this mechanism. This triggered a transition from stable bridging to rapid caving propagation, highlighting the non-linear nature of subsidence where specific geometric combinations can induce major instability.

The influence of panel width (Fig. 6) exhibits a strong positive correlation. Increasing width from 55 m to 100 m significantly amplifies subsidence magnitude and expands the lateral trough. Consistent with the field validation, all profiles in Fig. 6 display the characteristic asymmetry, where the point of maximum subsidence shifts distinctly toward the down-dip direction relative to the geometric center line. Conversely, panel depth (Fig. 7) shows an inverse relationship. Increasing depth reduces Smax significantly. Thicker overburden facilitates the formation of a stable pressure arch, effectively redistributing vertical loads to abutments. Furthermore, deformation energy is dissipated over a larger rock volume in deeper scenarios, resulting in a reduced and more dispersed surface manifestation. Finally, extraction height (Fig. 8) demonstrates a direct correlation. Higher extraction generates a larger void volume. Specifically, a 10 m height creates a void that exceeds the immediate bulking capacity of the collapsed roof, allowing deformation to propagate extensively to the surface. In contrast, voids from lower extraction heights are more readily filled by expanded caved material, constraining upward propagation.

Table 3. Numerical simulation results

Model	Width (m)	Depth (m)	Height (m)	Vertical displacement (m)
1	55	145	5	0.0096
2	55	200	3	0.0118
3	55	200	5	0.0186
4	70	200	3	0.0201
5	55	145	3	0.0203
6	70	200	5	0.0281
7	55	100	3	0.0326
8	100	100	3	0.0329
9	70	145	3	0.0343
10	100	200	3	0.0391
11	55	100	5	0.0464
12	70	145	5	0.0496
13	70	100	3	0.0549
14	100	200	5	0.0564
15	55	200	10	0.0604
16	100	145	3	0.0606
17	55	145	10	0.0729
18	70	100	5	0.0739
19	100	145	10	0.0817
20	100	145	5	0.0979
21	70	200	10	0.0979
22	70	100	10	0.1002
23	55	100	10	0.1117
24	100	100	5	0.1425
25	70	145	10	0.1458
26	100	200	10	0.1925
27	100	100	10	1.65

5. DISCUSSION

5.1 Strata Propagation Mechanism

The displacement of the subsidence trough toward the down-dip direction is primarily governed by the strata propagation trajectory. Unlike horizontal strata where caving propagates vertically, deformation in

dipping formations tends to occur perpendicular to the bedding planes. This kinematic constraint introduces a significant horizontal component to the overburden movement, effectively skewing the principal direction of failure.

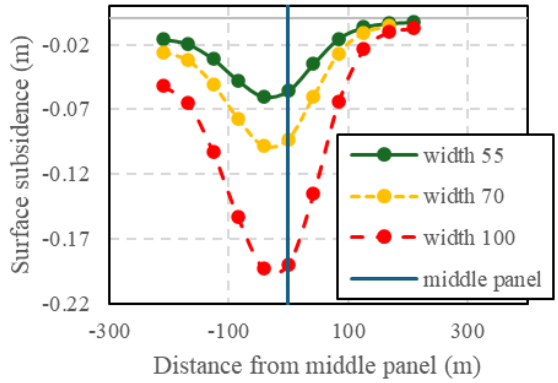

Fig. 6 The influence of panel width on surface subsidence

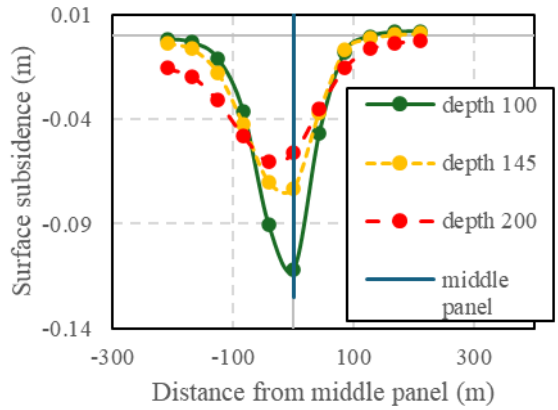

Fig. 7 The relationship between panel depth and surface subsidence

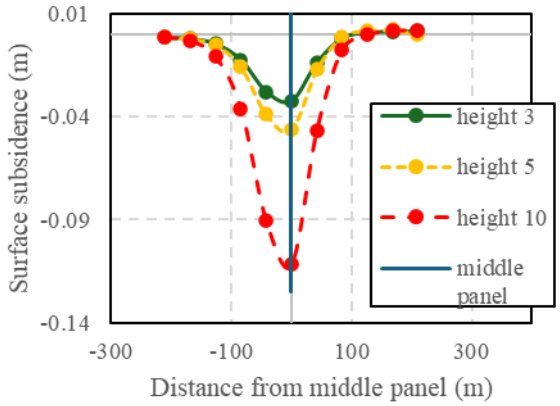

Fig. 8 The influence of panel height on surface subsidence

Consequently, the entire subsidence basin is not centered over the extraction panel but shifts laterally. This behavior induces a marked asymmetry in the angle of draw, which extends further on the down-dip side while contracting on the up-dip side. As a result, both the limit of subsidence and the locus of Smax are displaced toward the down-dip direction, consistent with the concept that gravity acts on the dipping strata to facilitate movement along the structural decline.

5.2 Statistical Correlation of Panel Geometry and Subsidence Magnitude

Pearson correlation analysis was conducted to quantify the influence of geometric parameters on absolute maximum subsidence. The results identify panel height as the governing variable, exhibiting a strong positive correlation ($\rho = 0.671$). This confirms that extraction thickness acts as the primary intensifier of vertical displacement. Panel width demonstrates a moderate positive influence ($\rho = 0.395$), affecting both magnitude and the lateral extent of the trough. Conversely, panel depth displays a weak inverse relationship ($\rho = -0.141$), functioning as a minor attenuating factor due to the increased bridging capacity of the thicker overburden strata.

5.3 Practical Implications for Subsidence Management in Inclined Seams

The identified shift in the subsidence trough offers critical guidelines for operational management. Since the influence zone extends significantly down-dip, traditional symmetrical monitoring layouts are inadequate. Instead, monitoring networks should be designed asymmetrically, extending further in the down-dip direction to effectively capture the shifted deformation zone. Furthermore, risk assessment protocols must recognize that surface structures on the down-dip side face higher exposure than equidistant structures on the up-dip side. Consequently, safety pillar design and hazard zonation should incorporate this inclination-induced offset to ensure adequate protection.

5.4 Limitations and Future Research Directions

Specific constraints define the scope of this study. Geometrically, the fixed inclination (16°) and panel length (110 m) reflect specific operational conditions in East Kalimantan, rendering quantitative results site-specific. However, the observed qualitative trend—specifically the subsidence shift toward the down-dip direction—is driven by fundamental gravitational forces and remains generally applicable. Regarding material behavior, the simplified linear-elastic goaf and elastoplastic model capture the final equilibrium asymmetry but exclude non-linear gob compaction and time-dependent creep. Future research should therefore incorporate variable bulking factors, goaf stiffness sensitivity, and visco-elastic models to refine magnitude predictions and capture dynamic subsidence evolution across a broader range of dip angles.

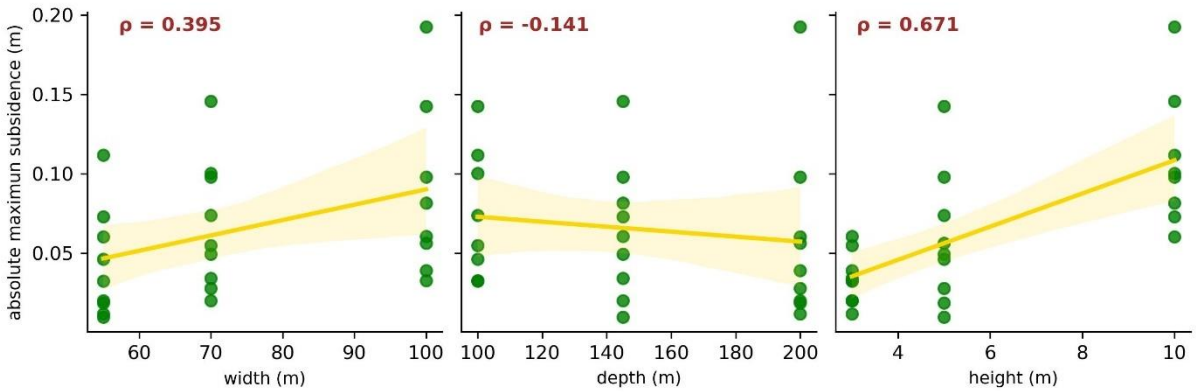

Fig. 9 The correlation analysis between absolute maximum subsidence and the panel geometry parameters

6. CONCLUSIONS

This study investigated surface subsidence in an inclined coal seam (16°) in East Kalimantan using 3D numerical modeling. Results indicate that seam inclination significantly alters trough morphology, shifting the locus of maximum subsidence toward the down-dip direction, while the profile exhibits a steeper gradient on the up-dip side. Parametric analysis identifies extraction height as the dominant factor governing magnitude ($\rho = 0.671$), followed by panel width, while panel depth acts as a minor natural attenuator.

Operationally, these findings highlight the risks of applying conventional flat-seam assumptions to Indonesian mining conditions. Monitoring networks should therefore adopt an asymmetrical layout extending further in the down-dip direction to capture the shifted deformation zone. While constrained by the specific dip angle and elastic goaf assumptions, these results provide a critical baseline for inclined seams. Future research should extend this framework by incorporating non-linear goaf compaction and visco-elastic models to refine absolute magnitude predictions and capture the temporal evolution of ground movement.

7. ACKNOWLEDGEMENTS

This research was supported by the JSPS KAKENHI Grant Number JP25K01715. The authors gratefully acknowledge their support.

8. REFERENCES

1. Gallowa D., Jones D.R., and Ingebritsen S.E., Land Subsidence in the United States. US Geological Survey Circular, 2000, no. 1182, pp. 1–175.
2. Erkens G., Bucx T., Dam R., De Lange G., and Lambert J., Sinking Coastal Cities. Proceedings of the International Association of Hydrological Sciences, 2015, vol. 372, no. April 2016, pp. 189–198.
3. Ramirez R.A., Abdullah R. E. E., and Rubio C. J. P., S1-Psinsar Monitoring and Hyperbolic Modeling of Nonlinear Ground Subsidence in Naga City, Cebu Island in the Philippines. International Journal of GEOMATE, 2022, vol. 23, no. 100, pp. 102–109. https://doi.org/10.21660/2022.100.g12121
4. Kozhas A., Mukhamejanova A., Toleubayeva S., Tleulenova G., and Tleubayeva A., Method of Predictive Calculation of the Earth'S Surface Subsidence for Protecting Railways Against Underworking. International Journal of GEOMATE, 2023, vol. 25, no. 107, pp. 95–106. https://doi.org/10.21660/2023.107.3789
5. Cui X.M., Li C.Y., Hu Q.F., and Miao X.X., Prediction of Surface Subsidence Due To Underground Mining Based on the Zenith Angle. International Journal of Rock Mechanics and Mining Sciences, 2013, vol. 60, pp. 246–252. http://dx.doi.org/10.1016/j.ijrmms.2012.12.036
6. Jung Y.B., Song W.K., Cheon D.S., Lee D.K., and Park J.Y., Simple Method For the Identification of Subsidence Susceptibility Above Underground Coal Mines in Korea. Engineering Geology, 2014, vol. 178, pp. 121–131. http://dx.doi.org/10.1016/j.enggeo.2014.06.006
7. Karian T., Kramadibrata S., Sulistianto B., Shimada H., Sasaoka T., Wahyudi S., and Matsui K., Surface Subsidence Prediction of Longwall Underground Coal Mining Prototype by Using Numerical and Empirical Method. ISRM International Symposium - 8th Asian Rock Mechanics Symposium ARMS8, 2014, no. October, pp. 2571–2580.
8. McCay A.T., Valyrakis M., and Younger P. L., A Meta-analysis of Coal Mining Induced Subsidence Data and Implications For Their Use in the Carbon Industry. International Journal of

Coal Geology, 2018, vol. 192, no. April, pp. 91–101. https://doi.org/10.1016/j.coal.2018.03.013
9. Derbin Y.G., Walker J., Wanatowski D., and Marshall A. M., Numerical Simulation of Surface Subsidence After the Collapse of a Mine. Springer, Cham, 2019, pp. 80 ‑ 97. https://doi.org/10.1007/978-3-319-95645-9_9
10. Jeon B., Jeon S., Kim J., and Kim T.H., Numerical Evaluation of Affecting Parameters of Surface Subsidence in Abandoned Mine Areas. Geosystem Engineering, 2012, vol. 15, no. 4, pp. 299–304. http://dx.doi.org/10.1080/12269328.2012.706386
11. Jeon B., Jeong H., Cho, S., and Jeon S., Assessment of Subsidence Hazard in Abandoned Mine Area Using Strength Reduction Method. KSCE Journal of Civil Engineering, 2022, vol. 26, no. 10, pp. 4338–4358. http://dx.doi.org/10.1007/s12205-022-2408-z
12. Xu N., Kulatilake P. H. S. W., Tian H., Wu X., Nan Y., and Wei T., Surface Subsidence Prediction for the Wutong Mine Using a 3-D Finite Difference Method. Computers and Geotechnics, 2013, vol. 48, pp. 134–145.
13. Alejano L., Ramírez-Oyanguren P., and Taboada J., FDM Predictive Methodology for Subsidence Due to Flat and Inclined Coal Seam Mining. International Journal of Rock Mechanics and Mining Sciences, 1999, vol. 36, no. 4, pp. 475–491. https://doi.org/10.1016/S0148-9062(99)00022-4
14. Yavuz H., An Estimation Method for Cover Pressure Re-establishment Distance and Pressure Distribution in the Goaf of Longwall Coal Mines. International Journal of Rock Mechanics and Mining Sciences, 2004, vol. 41, no. 2, pp. 193–205.
15. Cheng Y. M., Wang J. A., Xie G. X., and Wei W.B., Three-Dimensional Analysis of Coal Barrier Pillars in Tailgate Area Adjacent to the Fully Mechanized Top Caving Mining Face. International Journal of Rock Mechanics and Mining Sciences, 2010, vol. 47, no. 8, pp. 1372–1383. http://dx.doi.org/10.1016/j.ijrmms.2010.08.008
16. Pongpanya P., Sasaoka T., and Shimada H., Prediction of Multi-Seam Mining-Induced Surface Subsidence in Underground Coal Mine In Indonesia. ASEAN Engineering Journal. 2022, vol. 2, no.2, pp. 169–183. https://doi.org/10.11113/aenj.V12.17263
17. Peng S.S., Longwall Mining; Third Edition,. CRC Press/Balkema, Netherlands, 2020, pp.46-48. https://doi.org/10.1201/9780429260049
18. Zakri R.S., Wattimena R.K., Prassetyo S. H., and Karian T., Influence of Mining Depth and Panel Length in Longwall Underground Coal Mining on the Distribution of Principal Stresses Along the Barrier Pillars. IOP Conference Series: Earth and Environmental Science, 2024, vol. 1422, no. 1. https://doi.org/10.1088/1755-1315/1422/1/012014
19. Sasaoka T., Mao P., Shimada H., Hamanaka A., and Oya J., Numerical Analysis of Longwall Gate-entry Stability Under Weak Geological Condition: A Case Study of An Indonesian Coal Mine. Energies, 2020, vol. 13, no. 18, 4710. https://doi.org/10.3390/en13184710